Direct evidence for Sb as a Zn site impurity in ZnO

U. Wahl,[1,2,a)] J. G. Correia,[1,2,3] T. Mendonça,[4] and S. Decoster[5]
[1]*Instituto Tecnológico e Nuclear, Estrada Nacional 10, 2686-953 Sacavém, Portugal*
[2]*Centro de Física Nuclear da Universidade de Lisboa, Avenida Professor Gama Pinto 2, 1649-003 Lisboa, Portugal*
[3]*CERN-PH, 1211 Geneva 23, Switzerland*
[4]*Departamento de Física, Universidade do Porto, Rua do Campo Alegre 687, 4169-007 Porto, Portugal*
[5]*Instituut voor Kern-en Stralingsfysica and INPAC, KU Leuven, Celestijnenlaan 200D, 3001 Leuven, Belgium*

(Received 28 April 2009; accepted 26 May 2009; published online 29 June 2009)

The lattice location of ion implanted antimony in zinc oxide has been determined by means of β^- emission channeling from the radioactive ^{124}Sb isotope. Following 30 keV implantation of ^{124}Sb into a single-crystalline ZnO sample to a fluence of 1×10^{14} cm^{-2}, the angular-dependent emission rate of β^- particles around several crystallographic directions was measured with a position-sensitive Si detector. The majority of Sb was found to occupy Zn sites, with the possible fraction on O sites being at maximum 5%–6%. © *2009 American Institute of Physics*.
[DOI: 10.1063/1.3159474]

To date, the group V element antimony is one of the elements which have been used as *p*-type dopants in the II-VI semiconductor zinc oxide, the others being N, P, and As (cf. Ref. 1 and references therein). In the case of Sb, following the report of Sb-doped *p*-type ZnO by Aoki *et al.*[2] in 2002 and further work by other authors,[3–6] recently the realization of a wide range of optoelectronic devices incorporating *p*-ZnO:Sb layers have been reported, including homojunction and heterojunction photodiodes,[7,8] ultraviolet (UV) light emitting diodes,[9–12] and UV lasers.[13]

While technological applications of *p*-type ZnO seem thus to have come within reach, the nature of the acceptors in P, As or Sb-doped ZnO continues to be disputed in the literature. From a simple viewpoint of chemical bonding, the substitution of O^{2-} cations in ZnO by P^{3-}, As^{3-} or Sb^{3-} should create fully ionized acceptors. However, due to the large mismatch of the ionic radii of P^{3-} (2.12 Å), As^{3-} (2.22 Å), and Sb^{3-} (2.45 Å) with the ionic radius of O^{2-} (1.38 Å), it was argued that those impurities should have a low solubility substituting for O.[14] Moreover, theory suggests that the energy levels of P, As, and Sb replacing O are located deep in the band gap of ZnO.[15,16] In order to explain the *p*-type character of ZnO following As and Sb doping it was suggested that the acceptor action is actually due to As_{Zn}-$2V_{Zn}$ or Sb_{Zn}-$2V_{Zn}$ complexes, where an As or Sb atom occupies a Zn "antisite" and is decorated with two Zn vacancies.[16–19] However, a complex acceptor model for P, As or Sb in ZnO is strongly disputed by some authors.[20–24]

Obviously knowledge on the lattice location of the group V elements in ZnO is crucial in order to assess the related mechanism of *p*-type doping. We have previously determined the lattice sites of ion implanted As by means of conversion electron emission channeling from radioactive ^{73}As (Refs. 25–27) and found that As does not occupy substitutional O sites but mostly substitutional Zn sites. In this work we report on the lattice location of ion implanted radioactive ^{124}Sb ($t_{1/2}$=60.3 d) using β^- emission channeling and we present direct experimental evidence that Sb preferentially occupies Zn sites. Emission channeling[28] is based on the fact that charged particles from nuclear decay (α, β^-, β^+, and conversion electrons) experience channeling or blocking effects along major crystallographic axes and planes. The resulting anisotropic emission yield patterns from the crystal surface characterize the lattice site occupied by the probe atoms prior to the decay.

The production and implantation of ^{124}Sb were performed at CERN's on-line isotope separator facility ISOLDE, where beams of radioactive Sb ions are produced by nuclear reactions of a 1 GeV proton beam with UC_2 targets followed by resonant laser ionization.[29] The sample was a single crystal of ZnO grown by the hydrothermal method (commercially available from CrysTec GmbH) into which ^{124}Sb was implanted at room temperature with 30 keV energy to a fluence of 1×10^{14} cm^{-2}. The Sb depth profile corresponding to these implantation conditions is centered at a depth of 106 Å, with a straggling of 41 Å. The isotope ^{124}Sb decays by the emission of β^- particles with an end point energy of 2.30 MeV into stable ^{124}Te, the mean value of the β^- energy being 378 keV. The angular emission patterns of the β^- particles in the energy window above 35 keV were recorded around the [0001], [$\bar{1}$102], [$\bar{1}$101], and [$\bar{2}$113] directions at room temperature by means of a position-sensitive Si detector,[30] in the as-implanted state and following 10-min annealing steps at 200, 600, 800, and 900 °C under vacuum below 10^{-5} mbar. The angular resolution due to the size of the implanted spot on the sample and the position resolution of the detector was ~0.16° (standard deviation).

The evaluation of the probe atom lattice location was performed by quantitatively comparing the experimental patterns with theoretical ones calculated for ^{124}Sb on various different lattice sites, using the two-dimensional fit procedure outlined in Ref. 30. In the fit procedure, we considered theoretical patterns resulting from emitter atoms at substitutional Zn (S_{Zn}) and substitutional O (S_O) sites with varying isotropic root-mean-square (rms) Gaussian displacements, the main interstitial sites *T* and O (cf. Refs. 25 and 27), and a diversity of interstitial sites resulting from displacements along or off the *c* axis. The theoretical β^- emission channeling patterns were calculated by means of the "many beam"

a)Electronic mail: uwahl@itn.pt.

 © 2009 American Institute of Physics

Downloaded 30 Jun 2009 to 134.58.253.57. Redistribution subject to AIP license or copyright; see http://apl.aip.org/apl/copyright.jsp

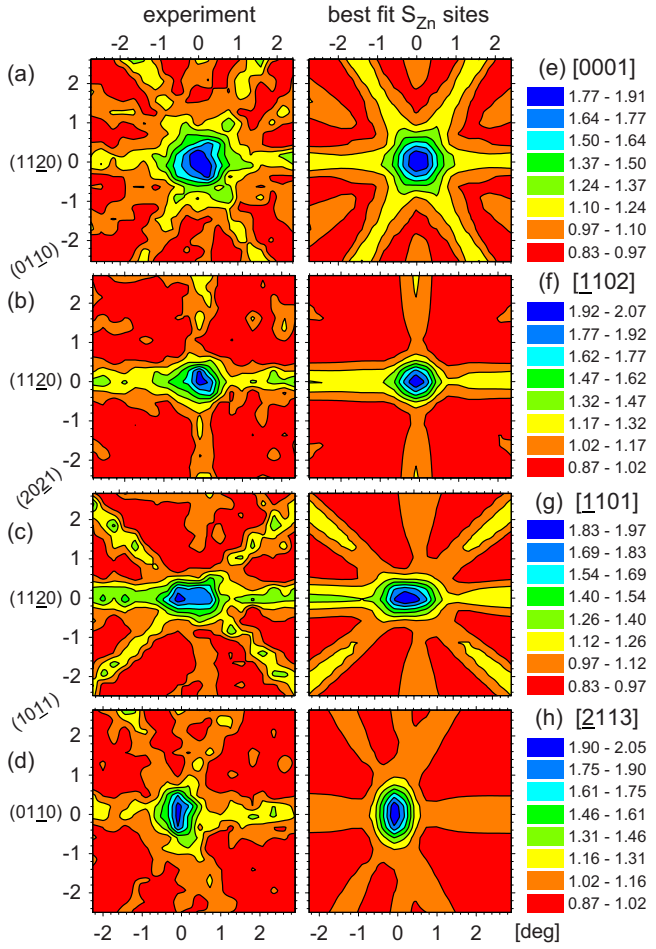

FIG. 1. (Color online) Angular distribution of normalized β^- emission yields from ^{124}Sb in ZnO following 600 °C annealing around the (a) [0001], (b) [1102], (c) [1101], and (d) [2113] axis. [(e)–(h)]: Best fits of the channeling patterns corresponding to 70% of ^{124}Sb aligned with the *c* axis, and 54%, 61%, and 64% at substitutional S_{Zn} sites, respectively.

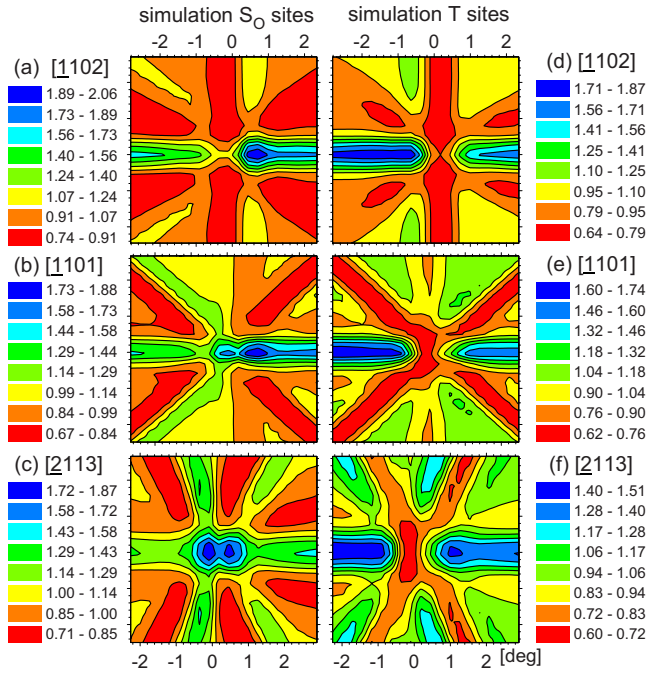

FIG. 2. (Color online) Theoretical emission channeling patterns for 100% of ^{124}Sb emitter atoms on substitutional oxygen (S_O) sites (a)–(c) and for 100% on interstitial *T* sites (d)–(f).

theory of electron diffraction in single crystals.[28] The continuous electron spectrum from the β^- decay was approximated in the calculations by a histogram with step widths of 25 keV electron energy up to 800 keV, of 50 keV up to 1.4 MeV, and of 100 keV up to 2.3 MeV. The number of beams used was 16 up to 725 keV electron energy, 20 up to 950 keV, and 24 at all higher energies. Details with respect to the structural properties of ZnO used in the simulations have been given previously.[31] The experimental patterns were corrected by subtracting an isotropic background contribution of 49% resulting from electrons that have been backscattered into the detector from inside the sample or by parts of the vacuum setup. This background contribution was estimated by means of Monte Carlo simulations based on the GEANT4 code,[32] taking into account the elemental composition and geometrical features of the sample, the sample holder, and the vacuum setup, as well as the electron energy distribution resulting from the β^- spectrum of ^{124}Sb.

The experimental β^- emission patterns along the [0001], [1102], [1101], and [2113] directions, following 600 °C vacuum annealing, are shown in Figs. 1(a)–1(d). The channeling effect along [0001] [Fig. 1(a)] indicates that the majority of the ^{124}Sb emitter atoms are located along the *c*-axis atomic rows. Fitting this experimental pattern by allowing only for emitter atoms with positions centered within the *c*-axis rows and on random sites, resulted in the theoretical pattern shown in Fig. 1(e), which corresponds to 70% of ^{124}Sb along the *c* axis with a rms displacement of $u_1(^{124}\text{Sb}) = 0.14$ Å perpendicular to this direction. Note that this does not yet allow distinguishing between a preference for S_{Zn} and S_O sites since both are aligned with the [0001] axis, along with a number of interstitial sites, e.g., the *T* sites. The site preference of Sb becomes obvious when the [1102], [1101], and [2113] experimental patterns are fitted in a similar way, however, in this case only allowing for emitter atoms on substitutional Zn and random sites. The resulting best fit theoretical patterns are shown in Figs. 1(f)–1(h) and correspond to 54%, 61%, and 64% at substitutional S_{Zn} sites with perpendicular ^{124}Sb rms displacements of 0.10, 0.14, and 0.19 Å, respectively.

The fit value for the fraction of Sb atoms aligned with the *c* axis is approximately 6% to 16% larger than those for Sb on Zn sites. This could indicate that some Sb atoms are located on sites that are aligned with the *c* axis but are different from S_{Zn} sites, e.g., S_O or *T* sites. In order to test this hypothesis, fits were carried out for the [1102], [1101], and [2113] patterns, allowing for additional fractions on S_O or *T* sites. Note that for these directions emitter atoms on S_O or *T* sites would produce channeling patterns (Fig. 2) that are distinctively different from S_{Zn} site patterns. However, this resulted only in minor improvements in the quality of fit, with the additional ^{124}Sb fractions on S_O, *T* or other sites being in the 5%–6% range at maximum. Figure 3(a) shows the fitted fractions of Sb emitter atoms as a function of annealing temperature when both S_{Zn} and S_O sites were allowed in the fit. The fitted fraction for Sb on oxygen sites is never larger than 5%–6%, which is at the detection limit of the technique for this isotope (note that around half of the count rate resulted from scattered electrons). On the other hand, the fitted fraction of Sb on Zn sites is around 50%–60% for annealing temperatures up to 600 °C and then drops to 20% following

Downloaded 30 Jun 2009 to 134.58.253.57. Redistribution subject to AIP license or copyright; see http://apl.aip.org/apl/copyright.jsp

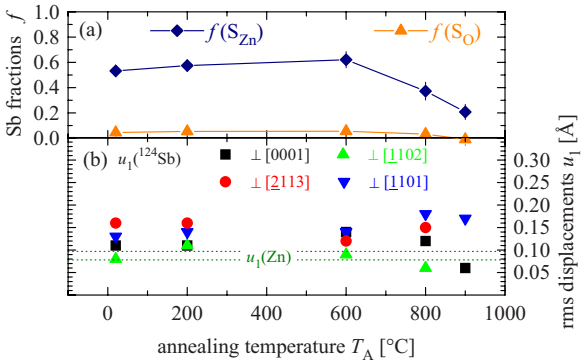

FIG. 3. (Color online) (a) Fractions of ^{124}Sb on substitutional Zn sites and possible fractions on substitutional O sites as a function of annealing temperature. (b) The best fit values for the rms displacements of the ^{124}Sb emitter atoms from ideal S_{Zn} sites, perpendicular to the four measured crystallographic directions. The two dotted lines indicate the range of room temperature rms displacements of Zn atoms.

900 °C vacuum annealing. The derived values for the rms displacements of ^{124}Sb [Fig. 3(b)] are generally somewhat larger but close to those for Zn atoms at room temperature, where reports in the literature vary between 0.078 and 0.097 Å. We interpret the decrease of the fraction of Sb on Zn sites following 800 and 900 °C annealing to be a consequence of the onset of Sb migration. This interpretation is supported by the fact that experiments where the diffusion of implanted Sb in ZnO was studied by means of secondary ion mass spectroscopy[33] observed slight changes in the implanted profiles for annealing temperatures at 800 °C or above. If Sb atoms are able to migrate, they may either pair with other defects resulting from the implantation process or from the vacuum annealing and thus be incorporated on random sites, or the implantation profile may substantially change, resulting in an increase of dechanneled electrons.

The lattice location of ^{124}Sb is in many respects similar to our previous results on implanted ^{73}As in ZnO,[25–27] where we found 70%–90% of As on S_{Zn} sites with the fraction on S_O sites being less than a few percent. While the fraction of ^{73}As on S_{Zn} sites also decreased following 900 °C vacuum annealing, it was possible to identify that ~30% of As was relocated to sites close to the interstitial *T* position. In comparison to ^{73}As, the experiments with ^{124}Sb could only be analyzed assuming a relatively high fraction (>40%) on random sites. However, we believe that this may be the consequence of an underestimation of the background correction resulting from the scattering of high-energy electrons. While the background correction for the β^- emitter ^{124}Sb relies on simulation results using the GEANT4 code, the measured conversion electron energy spectrum of ^{73}As directly allows determining the amount of inelastically scattered electrons, which is a more reliable procedure.

Summarizing, our findings clearly establish the preference of Sb for Zn sites and show that the fraction of implanted Sb on oxygen sites is at maximum a few percent. It is hence doubtful whether Sb_O acceptors are responsible for the reported *p*-type character in Sb-doped ZnO.

We acknowledge the beam time provided by the ISOLDE collaboration and funding by the Portuguese Foundation for Science and Technology (FCT, Project Nos. PTDC/FIS/66262/2006 and CERN/FP/83506/2008) and the European Union Sixth Framework (RII3-EURONS Contract No. 506065). T.M. acknowledges her Ph.D. student fellowship by FCT and SD financial support from FWO Flanders.

[1] D. C. Look, B. Claflin, Y. I. Alivov, and S. J. Park, Phys. Status Solidi A **201**, 2203 (2004).
[2] T. Aoki, Y. Shimizu, A. Miyake, A. Nakamura, Y. Nakanishi, and Y. Hatanaka, Phys. Status Solidi B **229**, 911 (2002).
[3] F. X. Xiu, Z. Yang, L. J. Mandalapu, D. T. Zhao, J. L. Liu, and W. P. Beyermann, Appl. Phys. Lett. **87**, 152101 (2005).
[4] O. Lopatiuk-Tirpak, W. V. Schoenfeld, L. Chernyak, F. X. Xiu, J. L. Liu, S. Jang, F. Ren, S. J. Pearton, A. Osinsky, and P. Chow, Appl. Phys. Lett. **88**, 202110 (2006).
[5] X. Pan, Z. Ye, J. Li, X. Gu, Y. Zeng, H. He, L. Zhu, and Y. Che, Appl. Surf. Sci. **253**, 5067 (2007).
[6] E. Przeździecka, E. Kamińska, I. Pasternak, A. Piotrowska, and J. Kossut, Phys. Rev. B **76**, 193303 (2007).
[7] L. J. Mandalapu, Z. Yang, F. X. Xiu, D. T. Zhao, and J. L. Liu, Appl. Phys. Lett. **88**, 092103 (2006).
[8] L. J. Mandalapu, Z. Yang, F. X. Xiu, D. T. Zhao, and J. L. Liu, Appl. Phys. Lett. **88**, 112108 (2006).
[9] L. J. Mandalapu, Z. Yang, S. Chu, and J. L. Liu, Appl. Phys. Lett. **92**, 122101 (2008).
[10] S. Chu, J. H. Lim, L. J. Mandalapu, Z. Yang, L. Li, and J. L. Liu, Appl. Phys. Lett. **92**, 152103 (2008).
[11] J. Kong, S. Chu, M. Olmedo, L. Li, Z. Yang, and J. Liu, Appl. Phys. Lett. **93**, 132113 (2008).
[12] J. Z. Zhao, H. W. Liang, J. C. Sun, J. M. Bian, Q. J. Feng, L. Z. Hu, H. Q. Zhang, X. P. Liang, Y. M. Luo, and G. T. Du, J. Phys. D **41**, 195110 (2008).
[13] S. Chu, M. Olmedo, Z. Yang, J. Kong, and J. Liu, Appl. Phys. Lett. **93**, 181106 (2008).
[14] S. J. Pearton, D. P. Norton, K. Ip, Y. W. Heo, and T. Steiner, Prog. Mater. Sci. **50**, 293 (2005).
[15] C. H. Park, S. B. Zhang, and S. H. Wei, Phys. Rev. B **66**, 073202 (2002).
[16] S. Limpijumnong, S. B. Zhang, S. H. Wei, and C. H. Park, Phys. Rev. Lett. **92**, 155504 (2004).
[17] S. Limpijumnong, M. F. Smith, and S. B. Zhang, Appl. Phys. Lett. **89**, 222113 (2006).
[18] S. Limpijumnong, M. F. Smith, and S. B. Zhang, Appl. Phys. Lett. **92**, 236102 (2008).
[19] Y. Shen, L. Mi, X. Xu, J. Wu, P. Wang, Z. Ying, and N. Xu, Solid State Commun. **148**, 301 (2008).
[20] V. Vaithianathan, B. T. Lee, C. H. Chang, K. Asokan, and S. S. Kim, Appl. Phys. Lett. **88**, 112103 (2006).
[21] V. Vaithianathan, S. S. Kim, and K. Asokan, Appl. Phys. Lett. **92**, 236101 (2008).
[22] M. S. Oh, D. K. Hwang, Y. S. Choi, J. W. Kang, S. J. Park, C. S. Hwang, and K. I. Cho, Appl. Phys. Lett. **93**, 111905 (2008).
[23] F. C. Zhang, Z. Y. Zhang, W. H. Zhang, J. F. Yan, and J. N. Yun, Chin. Phys. Lett. **25**, 3735 (2008).
[24] V. Vaithianathan, K. Asokan, J. Y. Park, and S. S. Kim, Appl. Phys. A: Mater. Sci. Process. **94**, 995 (2009).
[25] U. Wahl, E. Rita, J. G. Correia, A. C. Marques, E. Alves, and J. C. Soares, and the ISOLDE Collaboration, Phys. Rev. Lett. **95**, 215503 (2005).
[26] U. Wahl, E. Rita, J. G. Correia, A. C. Marques, E. Alves, and J. C. Soares, and the ISOLDE Collaboration, Superlattices Microstruct. **42**, 8 (2007).
[27] U. Wahl, J. G. Correia, E. Rita, A. C. Marques, E. Alves, and J. C. Soares, and the ISOLDE Collaboration, Mater. Res. Soc. Symp. Proc. **994**, F01 (2007).
[28] H. Hofsäss and G. Lindner, Phys. Rep. **201**, 121 (1991).
[29] R. Catherall, V. N. Fedosseev, U. Köster, J. Lettry, G. Suberlucq, B. A. Marsh, and E. Tengborn, and the ISOLDE Collaboration, Rev. Sci. Instrum. **75**, 1614 (2004).
[30] U. Wahl, J. G. Correia, A. Czermak, S. G. Jahn, P. Jalocha, J. G. Marques, A. Rudge, F. Schopper, J. C. Soares, A. Vantomme, and P. Weilhammer, and the ISOLDE Collaboration, Nucl. Instrum. Methods Phys. Res. A **524**, 245 (2004).
[31] U. Wahl, E. Rita, J. G. Correia, E. Alves, and J. P. Araújo, and the ISOLDE Collaboration, Appl. Phys. Lett. **82**, 1173 (2003).
[32] S. Agostinelli *et al.*, Nucl. Instrum. Methods Phys. Res. A **506**, 250 (2003).
[33] T. M. Børseth, J. S. Christensen, K. Maknys, A. Hallén, B. G. Svensson, and A. Yu. Kuznetsov, Superlattices Microstruct. **38**, 464 (2005).

Downloaded 30 Jun 2009 to 134.58.253.57. Redistribution subject to AIP license or copyright; see http://apl.aip.org/apl/copyright.jsp